

Initial measurements of atmospheric parameters in a marine environment

Frida Strömqvist Vetelino^a, Cynthia Young^a, Kenneth Grant^b, Linda Wasiczko^c,
Harris Burris^d, Christopher Moore^c, Rita Mahon^e, Michele Suite^c, Kerry Corbett^b,
Bradley Clare^b, Charmaine Gilbreath^c and William Rabinovich^c

^a Department of Mathematics, University of Central Florida, Orlando, FL 32816;

^b Defence Science and Technology Organisation, Edinburgh, SA, 5111, Australia

^c U.S. Naval Research Laboratory, 4555 Overlook Ave. SW, Washington, DC 20375

^d Research Support Instruments, Inc., 4325-B Forbes Blvd, Lanham, MD 20706

^e The Titan Corporation, 11955 Freedom Drive, Reston, VA 20190

ABSTRACT

In April 2005, a laser propagation experiment was conducted over a 470m horizontal maritime path. Scintillation measurements of a divergent Gaussian beam wave were taken simultaneously for different receiver aperture sizes. Terrestrial scintillation theory combined with a numerical algorithm was used to infer the atmospheric parameters C_n^2 and l_0 from the optical maritime scintillation measurements. This paper presents the initial results.

1. INTRODUCTION

In April 2005, a laser propagation experiment was conducted over a 470m horizontal maritime path, located at the Naval Research Laboratory's (NRL's) facilities at the Chesapeake Bay, Maryland. Scintillation measurements of a divergent Gaussian beam wave were taken simultaneously for different receiver aperture sizes. Scintillation theory for Gaussian beam waves, recently developed by Andrews *et al* for terrestrial conditions,^{1,2} combined with a numerical algorithm was used to infer the refractive index structure constant C_n^2 and the inner scale of turbulence l_0 from the optical scintillation measurements. In this experiment, the scintillation data was collected under the conditions of weak optical turbulence. The proposed method of inferring atmospheric parameters can be extended into the moderate-to-strong fluctuation regime, in which case values of the outer scale of turbulence L_0 , as well as C_n^2 and l_0 , can be determined.³

This work contains the initial results of applying scintillation theory developed for terrestrial conditions to maritime scintillation data. The ultimate goal is to make corrections to the scintillation theory for maritime conditions and redo this analysis to determine the impact of such corrections.

2. INFERRING ATMOSPHERIC PARAMETERS FROM OPTICAL MEASUREMENTS

The goal of this work is to infer the refractive index structure parameter, C_n^2 , and the inner scale of turbulence, l_0 , from optical scintillation measurements taken under weak turbulence conditions in a marine environment. The scintillation index, defined as the normalized variance of the irradiance,

$$\sigma_I^2 = \frac{\langle I^2 \rangle}{\langle I \rangle^2} - 1, \quad (1)$$

where I represents the irradiance of the optical wave and $\langle \cdot \rangle$ denotes ensemble average, is known to be sensitive to both C_n^2 and l_0 under all conditions of optical turbulence. The outer scale of turbulence, L_0 , has a negligible effect on the scintillation index under weak irradiance fluctuations, but its influence begins to emerge as the strength of the irradiance fluctuations increases. Hence, scintillation measurements taken in the weak optical turbulence regime cannot be used to infer the outer scale.

Report Documentation Page

Form Approved
OMB No. 0704-0188

Public reporting burden for the collection of information is estimated to average 1 hour per response, including the time for reviewing instructions, searching existing data sources, gathering and maintaining the data needed, and completing and reviewing the collection of information. Send comments regarding this burden estimate or any other aspect of this collection of information, including suggestions for reducing this burden, to Washington Headquarters Services, Directorate for Information Operations and Reports, 1215 Jefferson Davis Highway, Suite 1204, Arlington VA 22202-4302. Respondents should be aware that notwithstanding any other provision of law, no person shall be subject to a penalty for failing to comply with a collection of information if it does not display a currently valid OMB control number.

1. REPORT DATE 2006		2. REPORT TYPE		3. DATES COVERED 00-00-2006 to 00-00-2006	
4. TITLE AND SUBTITLE Initial measurements of atmospheric parameters in a marine environment				5a. CONTRACT NUMBER	
				5b. GRANT NUMBER	
				5c. PROGRAM ELEMENT NUMBER	
6. AUTHOR(S)				5d. PROJECT NUMBER	
				5e. TASK NUMBER	
				5f. WORK UNIT NUMBER	
7. PERFORMING ORGANIZATION NAME(S) AND ADDRESS(ES) Naval Research Laboratory, 4555 Overlook Avenue, SW, Washington, DC, 20375				8. PERFORMING ORGANIZATION REPORT NUMBER	
9. SPONSORING/MONITORING AGENCY NAME(S) AND ADDRESS(ES)				10. SPONSOR/MONITOR'S ACRONYM(S)	
				11. SPONSOR/MONITOR'S REPORT NUMBER(S)	
12. DISTRIBUTION/AVAILABILITY STATEMENT Approved for public release; distribution unlimited					
13. SUPPLEMENTARY NOTES					
14. ABSTRACT					
15. SUBJECT TERMS					
16. SECURITY CLASSIFICATION OF:			17. LIMITATION OF ABSTRACT	18. NUMBER OF PAGES 10	19a. NAME OF RESPONSIBLE PERSON
a. REPORT unclassified	b. ABSTRACT unclassified	c. THIS PAGE unclassified			

When comparing theory with experimental data obtained with larger apertures, aperture averaging effects (a reduction in scintillation with increasing receiver aperture size) have to be taken into account. As a result, by ignoring outer scale effects, the theoretical expressions for the scintillation index, at a fixed range and wavelength, depend on three parameters, C_n^2 , l_0 and D ,

$$\sigma_I^2(l_0, C_n^2, D) = \exp\left[\sigma_{\ln x}^2(l_0, C_n^2, D) + \sigma_{\ln y}^2(l_0, C_n^2, D)\right] - 1, \quad (2)$$

where D denotes the diameter of the receiver aperture, and $\sigma_{\ln x}^2$ and $\sigma_{\ln y}^2$ are the large scale and small scale log-irradiance variances, respectively. Expressions for the log-irradiance variances are provided in Appendix A. By specifying two different collecting aperture sizes, D_1 and D_2 , and measuring the corresponding scintillation index experimentally, $\sigma_{I,\text{exp}}^2$, the result is a system of two nonlinear equations with two unknowns,

$$\sigma_I^2(l_0, C_n^2, D_j) = \sigma_{I,\text{exp}}^2(D_j), \quad j = 1, 2, \quad (3)$$

where l_0 and C_n^2 are the unknowns to be determined and $\sigma_I^2(l_0, C_n^2, D)$ is the theoretical scintillation index defined in (2).

Due to the complexity and nonlinearity of (3), the system was solved numerically. However, rather than solving the system of equations in (3) directly, the problem was rewritten as a minimization problem by introducing the function

$$f(l_0, C_n^2) = \sum_{j=1}^2 \left[\sigma_I^2(l_0, C_n^2, D_j) - \sigma_{I,\text{exp}}^2(D_j) \right]^2. \quad (4)$$

A customized Mathematica program based on the downhill Simplex method^{4,5} was used to find the l_0 and C_n^2 values that minimize $f(l_0, C_n^2)$ in (4). The downhill Simplex method is a multidimensional minimization algorithm that requires only function evaluations, not derivatives. The simplex is a geometrical figure consisting, in N dimensions, of $N+1$ points (vertices) and their interconnecting line segments. In two dimensions, the simplex is a triangle.⁴

In addition to an initial estimate, the downhill Simplex method requires N extra points to form the initial simplex. These points are determined by specifying the initial estimate, \mathbf{P}_0 , and an initial step-size, $\boldsymbol{\delta}$. Both \mathbf{P}_0 and $\boldsymbol{\delta}$ are N -dimensional vectors. The additional N points are then given by $\mathbf{P}_i = \mathbf{P}_0 + \delta_i \mathbf{e}_i$, where δ_i is the i^{th} element in the step-size vector $\boldsymbol{\delta}$ and \mathbf{e}_i is a unit vector. The algorithm moves the simplex downhill on the N -dimensional surface until it reaches a minimum, where the simplex contracts itself in all directions. The lowest point of the simplex is chosen as the solution of the minimization problem.⁴

The termination criterion for the Simplex method cannot be chosen to require a certain tolerance for a single independent variable. The algorithm can be programmed to terminate when either the decrease in the function value in one step is smaller than some tolerance, or the vector distance moved in one step becomes smaller than some tolerance. Due to the experimental error, the minimum value of (4) will most likely never be exactly zero. Therefore, it is better to use a termination criterion that depends on the variables, rather than the function value. Since the simplex contracts itself around a minimum, the ‘‘simplex size’’, defined as the sum of the Euclidean vector distance between all vertices in the simplex, was used as a termination criterion.

3. EXPERIMENT

3.1 Experimental setup

The experiment was conducted on April 6, 2005, at NRL’s facilities at the Chesapeake Bay, Maryland. A continuous wave laser operating at 1550nm was propagated horizontally 470m over open water between two piers. The beam divergence was estimated to be 3 mrad (full angle). The beam was detected by three germanium photodiodes of 1mm,

5mm and 13mm diameters (Judson J16TE2-8A6-RO1M, J16TE2-8A6-RO5M, J16TE1-P6-R13M-HS), respectively, and a 12.7cm diameter telescope (Maksutov-Cassegrain) combined with a germanium detector. To reduce background radiation, two 1550nm notch filters were placed in front of the 5mm and 13mm Ge detectors, and their field of view was limited by tubes of 2.54cm diameter and 45.72cm length. In order to receive signal on the 1mm Ge detector, no filter was used and the length of tube was reduced to 15.24cm. The telescope detector had neutral density filters placed in front of it.

Two tripods were used to hold the detectors, one with the 3 Ge-detectors and one with the telescope. All detectors were positioned about 3-4m above the water surface. Each of the three Ge-detectors was connected to a pre-amplifier (Judson PA-7-70), and the voltage signal was captured with a sampling rate of 10kHz by a data acquisition card (National Instruments PCI-6071E) and a custom-written LabVIEW software. Data was taken in 5 minute intervals and the background radiation was measured either before or after each run. During the data collection, the weather was sunny and very windy, with air temperatures in the range 15-20 °C.

3.2 Data analysis

A Matlab program was written to calculate the mean signal and the scintillation index for each detector and each minute of collected data. In order to obtain the true experimental scintillation index (SI), $\sigma_{I,\text{exp}}^2$, the background noise was subtracted from each data point. The background noise, \bar{V}_{BG} , was estimated to be the mean signal of the background measurement taken either before or after each 5-minute interval of collected data. Rather than subtracting \bar{V}_{BG} from each data point and recalculating the SI from the corrected raw data, the corrected SI can be calculated according to

$$\sigma_{I,\text{exp}}^2 = \frac{\sigma_{I,\text{data}}^2 (\bar{V}_{\text{data}})^2}{(\bar{V}_{\text{data}} - \bar{V}_{\text{BG}})^2}, \quad (5)$$

where $\sigma_{I,\text{data}}^2$ and \bar{V}_{data} are the SI and mean signal (voltage) calculated by the Matlab program for each minute of collected data. The average signal-to-noise ratio (SNR) for all data runs varied for the different detectors and is shown in Table 1. For the 5mm, 13mm and 12.7 cm apertures, the background correction resulted in a minor change in the scintillation index, making $\sigma_{I,\text{exp}}^2$ on average only 0.2%, 2% and 0.06% higher than $\sigma_{I,\text{data}}^2$, respectively. However, for the 1mm aperture, $\sigma_{I,\text{exp}}^2$ was more than 50% higher than $\sigma_{I,\text{data}}^2$. In addition, $\sigma_{I,\text{exp}}^2$ for the 1mm aperture was consistently lower than $\sigma_{I,\text{exp}}^2$ for the 5mm aperture, which is contradicting aperture averaging theory. Hence, the data from the 1mm could not be used.

Table 1.

Aperture diameter	SNR [dB]
1 mm	5.9
5 mm	30.5
13 mm	20.0
12.7 cm	35.6

Before applying the downhill Simplex method to minimize $f(l_0, C_n^2)$ in (4), the variables l_0 and C_n^2 had to be made comparable in size. Hence, l_0 was specified in mm and C_n^2 in $\text{m}^{-2/3}$ on a \log_{10} -scale. A general two dimensional vector was set to $\mathbf{V} = (l_0, \log_{10}[C_n^2])$, the initial step-size was set to $\delta = (1, 0.1)$ and the initial estimate was chosen as $\mathbf{P}_0 = (3, \log_{10}[C_n^2]_{\text{initial}})$. \mathbf{V} , \mathbf{P}_0 and δ all have units (mm, $\log_{10}[\text{m}^{-2/3}]$). $C_n^2]_{\text{initial}}$ was determined from the relation

$$C_n^2]_{\text{initial}} = \frac{1}{9.12} \ln(1 + \sigma_{I,\text{exp}}^2) D^{7/3} L^{-3} \quad (6)$$

where D is the receiver aperture diameter, L the propagation distance and $\sigma_{I,\text{exp}}^2$ is the experimental scintillation index associated with D . Eq. (6) provides a good estimate of C_n^2 for large apertures, so the data from the 12.7cm aperture was used to calculate $C_n^2]_{\text{initial}}$. The termination criterion was chosen as the “simplex size” $< 10^{-9}$. This value was chosen to ensure a unique solution.

A customized Mathematica program employing the downhill Simplex method was used to perform a minimization for each minute of data. Since scintillation data was available from three different receiver apertures (5mm, 13mm and

12.7cm diameter), but only two are required for the minimization, three different combinations of aperture sizes could be used to infer the atmospheric parameters. The numerical scheme was tested with simulation data, which showed that the solutions obtained from the 5mm and 13mm apertures were unstable, i.e. very sensitive to small changes in the scintillation data. Hence, this combination of aperture sizes was disregarded. Results for C_n^2 and inner scale were obtained with both the 5mm and 12.7cm apertures and the 13mm and 12.7cm apertures. In both cases, the separation in aperture size was large enough to ensure stable solutions of C_n^2 and l_0 .

4. RESULTS AND DISCUSSIONS

The downhill Simplex method converges to a unique solution of the atmospheric parameters (C_n^2 and l_0) which agree with our physical intuition, i.e. a C_n^2 -value in the range 10^{-14} - 10^{-13} $m^{-2/3}$ and l_0 of the size of a few millimeters. The inferred C_n^2 - and l_0 -values are displayed in Figs. 1 and 2, respectively, as a function of time of day. The displayed data is from April 6, 2005 and the results are shown for both the 13mm and 12.7cm apertures (gray) and the 5mm and 12.7cm apertures (black). The majority of the inferred l_0 -values lie between 1.5mm and 2.5mm. These low values of the inner scale of turbulence can be explained by the extremely windy conditions during the experiment, since the inner scale is known to be inversely related to the average wind speed. For some minutes of data, the numerical scheme resulted in inner scale values very close to zero and very high C_n^2 -results (on the order of 10^{-12} $m^{-2/3}$). These results do not make physical sense and should be disregarded. (The high C_n^2 - values are not shown in Fig. 1 since they lie outside the range of the majority of the data).

Fig. 3 shows a comparison of the inferred atmospheric parameters obtained with different combinations of receiver aperture sizes (13mm and 12.7cm apertures and the 5mm and 12.7cm apertures) for each minute of data. The few minutes with an inner scale solution close to zero have been omitted from Fig. 3. As shown in Fig. 3a, the C_n^2 - values inferred from the 5mm and 12.7cm apertures are consistently larger than those inferred from the 13mm and 12.7cm apertures. The absolute difference between the two C_n^2 - values is on average, for all data runs, $9 \cdot 10^{-15}$ $m^{-2/3}$. As shown in Fig. 3b, the two different combinations of aperture sizes yield almost identical values of the inner scale of turbulence. On average, for all data runs, the absolute difference of the two inferred inner scale solutions is 0.06mm.

The accuracy of the solution to the Downhill Simplex method is related to the success of the minimization of $f(l_0, C_n^2)$ in (4), i.e. how small the difference between the measured and the theoretical scintillation index is for each aperture size. The success of the minimization can be measured in terms of the error of the theoretical scintillation index relative to the measured scintillation index, which is shown for each aperture size in Fig. 4. The theoretical scintillation index is calculated by inserting the inferred C_n^2 - and l_0 -values into (2) for each receiver aperture size. Fig. 4a shows the relative error calculated with the atmospheric parameters inferred from the measured scintillation data from the 5mm and 12.7cm apertures, while Fig. 4b displays the same quantity obtained from the 13mm and 12.7cm apertures.

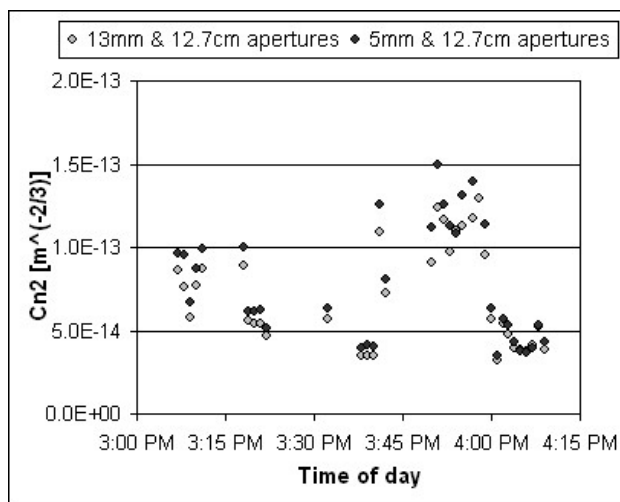


Fig. 1. The inferred C_n^2 - values as a function of time of day.

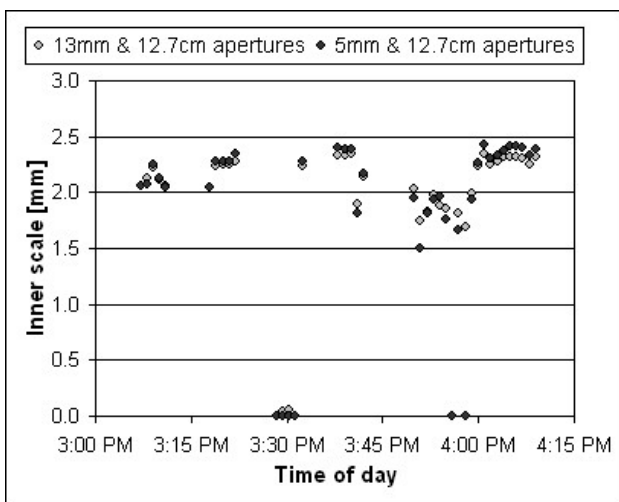
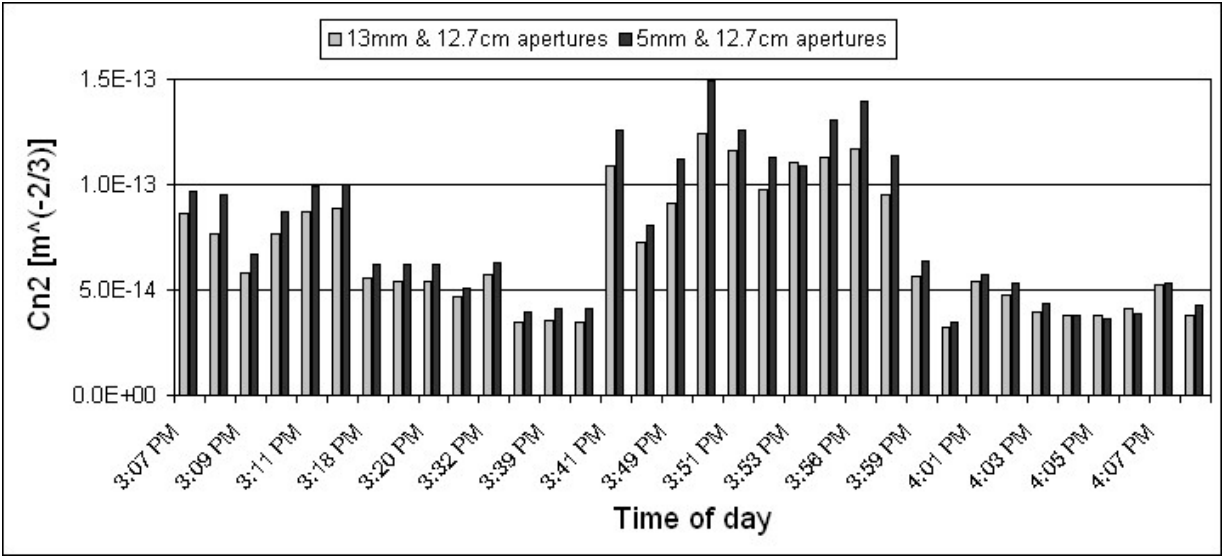
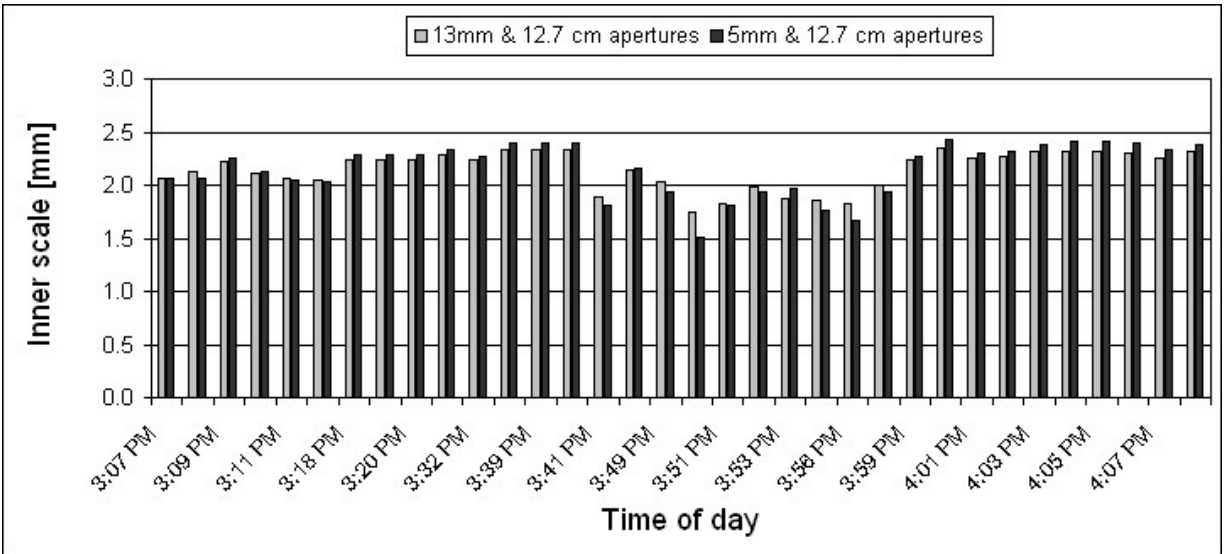


Fig. 2. The inferred l_0 - values as a function of time of day.

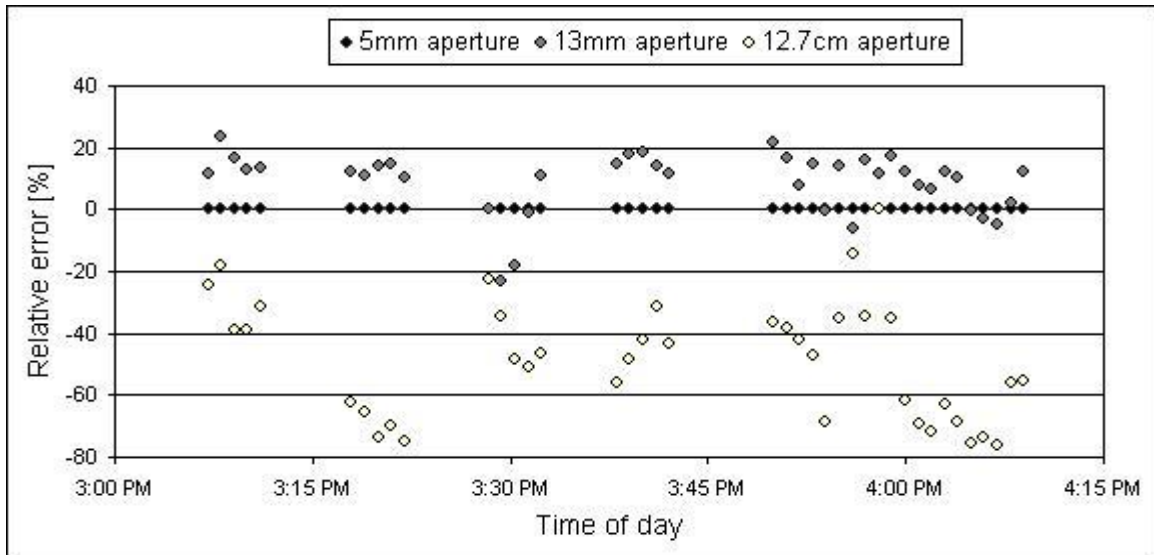


(a)

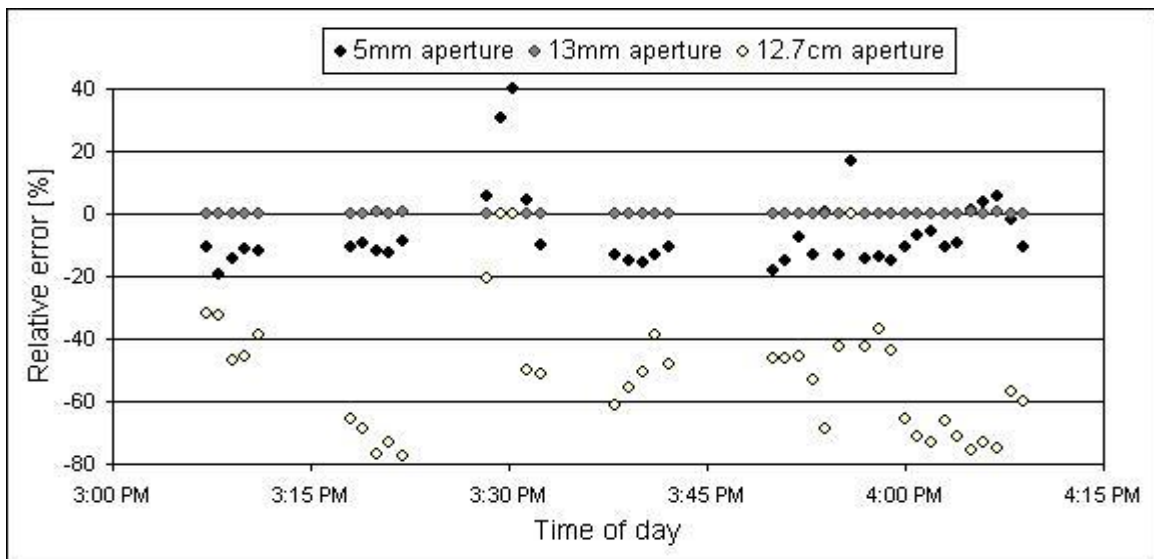


(b)

Fig. 3. Comparison between the inferred C_n^2 - values (a) and l_0 -values (b) obtained from the experimental data from either the 13mm and 12.7cm apertures or the 5mm and 12.7cm apertures.



(a)



(b)

Fig. 4. The relative error of the theoretical scintillation index (SI), compared to the experimental SI for all three aperture sizes. The theoretical SI for all three aperture sizes were calculated with the l_0 - and C_n^2 - values inferred from: (a) the 5mm and 12.7 cm apertures, (b) the 13mm and 12.7cm apertures.

As shown in Fig 4, the relative error for the smallest aperture used in the minimization, the 5mm aperture in Fig 4a and the 13mm aperture in Fig 4b, is almost zero, on average 0.08% and 0.16%, respectively, while the relative error for the 12.7cm aperture is significantly larger in both cases, on average 49% and 51%, respectively. The significant difference in the relative error for the two apertures used in the minimization occurs since the measured scintillation index for the smallest aperture is at least one order of magnitude larger than that for the 12.7cm aperture. Therefore, the relative error for the smallest aperture is favored in the minimization scheme and becomes almost zero. The large relative error for the 12.7cm aperture is a concern, however, since aperture averaging theory is not exact, a large relative error for the largest aperture is acceptable. The poor agreement between theory and measurement for the large aperture case may be due to the fact that the scintillation theory used was developed and validated for terrestrial conditions, while this experimental data was collected in a maritime environment. Further investigation is needed in order to determine if the scintillation theory needs to be modified for the maritime case.

The third relative error shown in Fig 4 displays the results for the aperture that was not used in the minimization scheme, the 13mm aperture in Fig 4a and the 5mm aperture in Fig 4b. This error shows how well the inferred atmospheric parameters can be used to predict the scintillation value at an arbitrary receiver aperture, compared to its measured value. On average, this relative error is 11.7% in Fig 4a and 11.8% in Fig 4b. In this context this is an acceptable error and justifies the use of this method to infer C_n^2 and the inner scale of turbulence. However, if the theory is adjusted to properly describe a maritime environment, improvements of these results may be expected.

5. SUMMARY

The purpose of the experiment, which was conducted in April 2005, was to obtain simultaneous scintillation measurements from two receivers of different aperture size and use the results to determine the atmospheric parameters C_n^2 and l_0 along a maritime propagation path. The parameters were inferred from a recently developed scintillation theory that is believed to be valid under weak to strong irradiance fluctuations. Receiver aperture sizes of 1mm, 5mm, 13mm and 12.7cm were placed at 470m from a laser source operating at 1.55 μ m, resulting in scintillation data from the weak regime of optical turbulence. These aperture sizes were not considered an optimal choice for this experiment but chosen primarily on the basis of availability.

Given the optical measurements from two of the receiver apertures, a numerical algorithm was developed in order to extract the atmospheric parameters from the complex theoretical expressions. Due to poor signal-to-noise ratio, the data from the 1mm receiver aperture was disregarded. The C_n^2 - and l_0 -values inferred from the scintillation data from the 5mm and 12.7cm apertures and the 13mm and 12.7cm aperture were in good agreement. The numerical scheme was not stable with respect to small changes in the experimental data for the 5mm and 13mm apertures. Hence, the latter combination of aperture sizes could not be used to infer the atmospheric parameters.

In conclusion, scintillation measurements from two receiver apertures, with a large separation in aperture size, can be used to infer path average values of C_n^2 and l_0 in the weak regime of optical turbulence in a maritime environment. Since the scintillation theory used was developed and validated for terrestrial conditions, further investigation is needed in order to determine if modifications are required for the maritime case.

The main advantage of the technique presented here is a straightforward extension into the moderate-to-strong fluctuation regime and long propagation paths. In the moderate-to-strong fluctuation regime, scintillation data from three different receiver aperture sizes are required and the outer scale of turbulence L_0 is obtained in addition to C_n^2 and l_0 . Existing methods of inferring inner scale values are limited to weak fluctuations conditions and, hence, short propagation paths.

This experiment was repeated in August 2005, when scintillation data was collected from seven different apertures. Further data analysis is in progress. Future work includes experiments over longer maritime propagation paths, in the moderate-to-strong optical turbulence, where path average values of all three atmospheric parameters (C_n^2 , l_0 and L_0) can be determined. In addition, further analysis on a maritime spectral model of the irradiance fluctuations and its impact on scintillation is necessary. If a modification of the existing terrestrial scintillation theory is required, this analysis should be repeated and comparisons made to the present results.

APPENDIX A

At the transmitter, a Gaussian beam wave is defined in terms of the beam radius W_0 and the phase front radius of curvature F_0 . These parameters are related to the (hard) transmitter aperture diameter d and the half-angle transmitter beam divergence θ_{div} , according to

$$W_0 = \frac{d}{2\sqrt{2}}, \quad F_0 = -\frac{W_0}{\theta_{div}}. \quad (\text{A.1})$$

A propagating beam is characterized by the beam parameters, which in the transmitting plane are defined by,⁶

$$\Theta_0 = 1 - \frac{L}{F_0}, \quad \Lambda_0 = \frac{2L}{kW_0}, \quad (\text{A.2})$$

where L is the propagation distance and k is the optical wave number. At the receiver, located at propagation distance L , the receiver beam parameters are defined by,⁶

$$\Theta = \frac{\Theta_0}{\Theta_0^2 + \Lambda_0^2}, \quad \bar{\Theta} = 1 - \Theta, \quad \Lambda = \frac{\Lambda_0}{\Theta_0^2 + \Lambda_0^2}. \quad (\text{A.3})$$

When outer scale effects are ignored, the theoretical expression for the scintillation index of a receiver with aperture diameter D is a function of C_n^2 , l_0 and D ,⁷

$$\sigma_I^2(l_0, C_n^2, D) = \exp\left[\sigma_{\ln x}^2(l_0, C_n^2, D) + \sigma_{\ln y}^2(l_0, C_n^2, D)\right] - 1, \quad (\text{A.4})$$

where $\sigma_{\ln x}^2$ and $\sigma_{\ln y}^2$ are large-scale and small-scale log-irradiance scintillation, respectively. For mathematical convenience, the following dimensionless quantities that depend on C_n^2 , l_0 and D are introduced⁷

$$Q_l(l_0) = \frac{10.89L}{kl_0^2}, \quad \sigma_1^2(C_n^2) = 1.23C_n^2k^{7/6}, \quad \Omega_G(D) = \frac{16L}{kD^2}, \quad (\text{A.5})$$

where L is the propagation distance and k is the optical wave number. For the on-axis portion of a Gaussian beam wave, $\sigma_{\ln x}^2$ is defined by⁷

$$\begin{aligned} \sigma_{\ln x}^2(l_0, C_n^2, D) = & 0.49\sigma_1^2\left(\frac{\Omega_G - \Lambda}{\Omega_G + \Lambda}\right)\left(\frac{1}{3} - \frac{1}{2}\bar{\Theta} + \frac{1}{5}\bar{\Theta}^2\right)\left(\frac{\eta_{xd}Q_l}{\eta_{xd} + Q_l}\right)^{7/6} \\ & \times \left[1 + 1.75\left(\frac{\eta_{xd}}{\eta_{xd} + Q_l}\right)^{1/2} - 0.25\left(\frac{\eta_{xd}}{\eta_{xd} + Q_l}\right)^{7/12}\right], \end{aligned} \quad (\text{A.6})$$

where

$$\eta_{xd}(l_0, C_n^2, D) = \frac{\eta_x}{1 + 0.40\eta_x(2 - \bar{\Theta})/(\Omega_G + \Lambda)}, \quad (\text{A.7})$$

$$\frac{1}{\eta_x(l_0, C_n^2)} = \frac{0.38}{1 - 3.21\bar{\Theta} + 5.29\bar{\Theta}^2} + 0.47\sigma_1^2 Q_l^{1/6} \left[\frac{\left(\frac{1}{3} - \frac{1}{2}\bar{\Theta} + \frac{1}{5}\bar{\Theta}^2\right)}{1.22\bar{\Theta}} \right], \quad (\text{A.8})$$

and $\bar{\Theta}$ and Λ are Gaussian beam parameters in the receiver plane. The small-scale log-irradiance scintillation, $\sigma_{\ln y}^2$, for a beam wave (on-axis), is defined by ⁷

$$\sigma_{\ln y}^2(l_0, C_n^2, D) = \frac{1.27\sigma_1^2 \eta_y^{-5/6}}{1 + 0.40\eta_y / (\Omega_G + \Lambda)}, \quad (\text{A.9})$$

where

$$\eta_y(l_0, C_n^2) = 3\left(\sigma_1^2 / \sigma_G^2\right)^{6/5} \left(1 + 0.65(\sigma_G^2)^{6/5}\right), \quad (\text{A.10})$$

$$\begin{aligned} \sigma_G^2(l_0, C_n^2) = & 3.86\sigma_1^2 \left\{ 0.40 \frac{\left[(1+2\Theta)^2 + (2\Lambda + 3/Q_l)^2\right]^{11/12}}{\left[(1+2\Theta)^2 + 4\Lambda^2\right]^{1/2}} \right. \\ & \times \left[\sin\left(\frac{11}{6}\varphi_2 + \varphi_1\right) + \frac{2.61 \sin\left(\frac{4}{3}\varphi_2 + \varphi_1\right)}{\left[(1+2\Theta)^2 Q_l^2 + (3+2\Lambda Q_l)^2\right]^{1/4}} - \frac{0.52 \sin\left(\frac{5}{4}\varphi_2 + \varphi_1\right)}{\left[(1+2\Theta)^2 Q_l^2 + (3+2\Lambda Q_l)^2\right]^{7/24}} \right] \\ & \left. - \frac{13.40\Lambda}{Q_l^{11/6} \left[(1+2\Theta)^2 + 4\Lambda^2\right]} - \frac{11}{6} \left[\left(\frac{1+0.31\Lambda Q_l}{Q_l}\right)^{5/6} + \frac{1.10(1+0.31\Lambda Q_l)^{1/3}}{Q_l^{5/6}} - \frac{0.19(1+0.24\Lambda Q_l)^{1/4}}{Q_l^{5/6}} \right] \right\}, \quad (\text{A.11}) \end{aligned}$$

and

$$\varphi_1 = \tan^{-1}\left(\frac{2\Lambda}{1+2\Theta}\right), \quad \varphi_2(l_0) = \tan^{-1}\left(\frac{(1+2\Theta)Q_l}{3+2\Lambda Q_l}\right), \quad (\text{A.12})$$

where $\bar{\Theta}$ and Λ are Gaussian beam parameters in the receiver plane.

ACKNOWLEDGMENTS

The work was supported in part by the Office of Naval Research, under Contract Number N00014-01-1-0412.

REFERENCES

1. L. C. Andrews, M. A. Al-Habash, C. Y. Hopen and R. L. Phillips, "Theory of optical scintillation: Gaussian-beam wave model," *Waves in Random Media* **11**, 271-291 (2001).
2. L. C. Andrews, R. L. Phillips and C. Y. Hopen, *Laser Beam Scintillation with Applications*, SPIE Optical Engineering Press, Bellingham, WA (2001).
3. F. Strömqvist Vetelino, B. Clare, K. Corbett, Young, K. Grant, and L. Andrews, "Characterizing the propagation path in moderate to strong optical turbulence", *Appl. Opt.* (in press)
4. "Downhill Simplex Method in Multidimensions," Ch. 10.4 in *Numerical Recipes in C: The art of scientific computing* (1988-1992),
<http://www.library.cornell.edu/nr/bookcpdf/c10-4.pdf>
5. Downhill Simplex Method, code for matlab:
<http://freehost26.websamba.com/zhanshan2002/matlab/simplex.html>
6. Section 1.3.1 , pp. 14-15 of Ref. 2
7. Section 6.5.3, p. 193 of Ref. 2